Development 137, 2167-2175 (2010) doi:10.1242/dev.051573

Mesoderm migration in *Drosophila* is a multi-step process requiring FGF signaling and integrin activity

Amy McMahon, Gregory T. Reeves, Willy Supatto* and Angelike Stathopoulos†

SUMMARY

Migration is a complex, dynamic process that has largely been studied using qualitative or static approaches. As technology has improved, we can now take quantitative approaches towards understanding cell migration using in vivo imaging and tracking analyses. In this manner, we have established a four-step model of mesoderm migration during *Drosophila* gastrulation: (I) mesodermal tube formation, (II) collapse of the mesoderm, (III) dorsal migration and spreading and (IV) monolayer formation. Our data provide evidence that these steps are temporally distinct and that each might require different chemical inputs. To support this, we analyzed the role of fibroblast growth factor (FGF) signaling, in particular the function of two *Drosophila* FGF ligands, Pyramus and Thisbe, during mesoderm migration. We determined that FGF signaling through both ligands controls movements in the radial direction. Thisbe is required for the initial collapse of the mesoderm onto the ectoderm, whereas both Pyramus and Thisbe are required for monolayer formation. In addition, we uncovered that the GTPase Rap1 regulates radial movement of cells and localization of the beta-integrin subunit, Myospheroid, which is also required for monolayer formation. Our analyses suggest that distinct signals influence particular movements, as we found that FGF signaling is involved in controlling collapse and monolayer formation but not dorsal movement, whereas integrins are required to support monolayer formation only and not earlier movements. Our work demonstrates that complex cell migration is not necessarily a fluid process, but suggests instead that different types of movements are directed by distinct inputs in a stepwise manner.

KEY WORDS: Fibroblast growth factors, Cell migration, Intercalation, In vivo imaging

INTRODUCTION

Controlled cell migration is an essential aspect of development in which cells relocate to respond to chemical signals and form structures (Lecaudey and Gilmour, 2006; Rorth, 2007; Montell, 2008; Ilina and Friedl, 2009). Aberrant migration, by contrast, can lead to diseases such as metastatic cancer (Deisboeck and Couzin, 2009; Friedl and Gilmour, 2009). As a result, studying the molecular and physical mechanisms that control migration is crucial for understanding both development and disease. Several models have been developed for examining different types of cell migration in vivo, such as the border cells in *Drosophila melanogaster* and the lateral line in *Danio rerio* for studying small group migrations, the neural crest cells in vertebrates for studying streaming, and wound healing for understanding sheet migration (Friedl and Gilmour, 2009; Rorth, 2009; Weijer, 2009). Here, we study the migration of the mesoderm during gastrulation in *Drosophila melanogaster* embryos as it is a tractable model for the collective migration of hundreds of mesenchymal cells that can be characterized by quantitative analysis (McMahon et al., 2008; Supatto et al., 2009).

Mesoderm migration in *Drosophila* involves several movements that transform a tube of cells into a monolayer; the completion of this migration is important for muscle and heart development (Leptin and Grunewald, 1990; Wilson and Leptin, 2000). First, the mesoderm invaginates by apical constriction to form an epithelial tube within the embryo. The mesoderm then undergoes an epithelial-to-mesenchymal transition (EMT) and collapse of the tube follows. Next, the collapsed cells spread dorsally along the ectoderm. Lastly, the mesoderm transforms from a multi-layer to a monolayer. This sequence of events has been described previously, but it was not known if these migratory actions were distinct or overlapping events. Furthermore, it has not been established whether particular biochemical signals are required to coordinate each event.

The most well-characterized molecular action during mesoderm migration is fibroblast growth factor (FGF) signaling (Wilson et al., 2005; Murray and Saint, 2007; McMahon et al., 2008; Kadam et al., 2009; Klingseisen et al., 2009). FGF signaling is essential in animals for both differentiation and migration (Thisse and Thisse, 2005). The FGF receptor (FGFR) Heartless (Htl) has been studied extensively in the context of mesoderm migration and differentiation (Beiman et al., 1996; Gisselbrecht et al., 1996) and has recently been shown definitively to control organized collapse of the mesodermal tube onto the underlying ectoderm during *Drosophila* gastrulation (McMahon et al., 2008). This organization helps maintain the collective behavior of the mesoderm, as the absence of Htl results in two behaviorally distinct cell populations. However, it remains unclear how the two ligands for Htl, the Fgf8-like Pyramus (Pyr) and Thisbe (Ths) proteins, contribute to this process.

In the *Drosophila* system, two different models have been presented regarding how Pyr and Ths activate the Htl receptor during mesoderm migration. The first model proposes that the ligands function redundantly and provide robustness, and the second suggests that the ligands activate the receptor differentially (Kadam et al., 2009; Klingseisen et al., 2009). These previous studies, which include our own previous work, addressed the role of Pyr and Ths ligands by extrapolating their functions during the

California Institute of Technology, Division of Biology MC 114-96, 1200 East California Boulevard, Pasadena, CA 91125, USA.

*Present address: Institut Jacques Monod, CNRS UMR 7592, Université Paris Diderot, Paris, France
†Author for correspondence (angelike@caltech.edu)

Accepted 27 April 2010

dynamic process of migration through examination of fixed tissues. Thus, it had yet to be determined definitively whether both Pyr and Ths are required for mesoderm migration during *Drosophila* gastrulation and, furthermore, whether the ligands regulate specific aspects of migration. Therefore, in this work, we explored the roles of Pyr and Ths during mesoderm migration using in vivo imaging and quantitative analyses; this general approach was used previously to decipher the FGFR mutant phenotype (McMahon et al., 2008; Supatto et al., 2009).

In addition to studying the two FGF ligands, we examined other molecules that could contribute to specific steps during mesoderm migration to test the hypothesis that mesoderm migration has temporally distinct inputs. We chose to examine the small GTPase Rap1 and integrins, as both have been implicated in migration and linked to FGF signaling (Mori et al., 2008; Carmona et al., 2009; Franzdottir et al., 2009). Rap1 has a demonstrated role in cell adhesion and migration in other systems (Huelsmann et al., 2006; Jeon et al., 2007; Boettner and Van Aelst, 2009). Rap1 regulates cell adhesion and migration, in part, through integrin activation (Reedquist et al., 2000; Kooistra et al., 2007; Boettner and Van Aelst, 2009; Carmona et al., 2009). Integrins are required for cell-cell junction formation and provide a physical link from these junctions to the actin cytoskeleton (Delon and Brown, 2007; Vicente-Manzanares et al., 2009). Of the two βPS subunits, only the βPS integrin, Myospheroid (Mys), is expressed in the *Drosophila* embryo during mesoderm migration (Leptin et al., 1989). Mys is involved in recruiting two alpha integrin subunits, αPS1 (Multiple edematous wings) and αPS2 (Inflated), to the cell membrane to form adhesion complexes that are important for cell migration and muscle attachment throughout *Drosophila* development (Leptin et al., 1989; Brown, 2000; O'Reilly et al., 2008). This evidence led us to investigate a role for Rap1 and Mys during mesoderm migration.

In this work, we present evidence that mesoderm migration is a multi-step process with temporally distinct migratory events. We show that movements in the radial direction, specifically collapse and monolayer formation, are controlled by FGF signaling. Dorsal movements appear to be FGF-independent. We find that the integrin subunit Mys is required only for monolayer formation. These results indicate that collapse, spreading and monolayer formation are not only temporally distinct, but also probably molecularly distinct.

MATERIALS AND METHODS

Fly stains and genetics

All crosses and strains were maintained at 25°C. The following lines were used: *yw*; *klar*^{1}; *htl*^{AB42}/TM3,ftz-*lacZ*; His2AV-GFP; *twi*-gal4; *twi-CD2*; *mys*^{1},FRT19A/FM7c,ftz-*lacZ* (Bloomington Stock Center); DfBSC25; *pyr*^{e02915}; *ths*^{e02026}; Df^{238} (Kadam et al., 2009); *pyr*^{18}; *ths*^{759} (Klingseisen et al., 2009); *Rap1*^{CD3} (Asha et al., 1999); *klar*^{1},His2AV-GFP; *klar*^{1},His2AV-GFP,*htl*^{AB42}/TM3,P[Dfd-GMR-nvYFP]3, Sb^{1} (McMahon et al., 2008). Wild-type refers to *yw* or His2AV-GFP flies. Germline clones were made for *Rap1*^{CD3} and *mys*^{1} using standard FRT-mediated germline clone methodology (Chou and Perrimon, 1996).

Morpholino design and injection

Anti-sense morpholinos were designed using the GeneTools Oligo Design and Ordering System (Gene Tools, LLC). The following sequences were used to make morpholinos: *pyr*, CATTGGGCATGAACTTGTGGAACAT; *ths*, GCAGTCTCTCTAACTGATTCGACAT; *Gal4*, CGATAGAAGACAGTAGCTTCATCTT; *mys*, TCGAGGATCATGGCTTTGGCGGTTA.

Morpholinos were resuspended in water to a final concentration of 1.5 to 2 mM. Filtered liquid green food coloring was added at 1/10 (vol/vol) to aid in visualization of injection. The injection protocol used was a modified version of Misquitta and Paterson (Misquitta and Paterson, 1999). *yw* or His2Av-GFP flies were collected in 15-minute intervals, washed with water to remove yeast and debris, lined up on a glass slide in a small volume of water and allowed to dry for 10 minutes before injection. Embryos were then covered with a thin layer of Halocarbon Oil 27 (Sigma-Aldrich). A morpholino or buffer alone was loaded into machine-pulled (Narishige) glass needles (FHC Inc.). To prevent needle clogging, morpholinos were heated to 65°C and allowed to cool at room temperature prior to being loaded into the needle. Morpholinos were injected into the ventral or dorsal side of the pre-cellularized embryo using a Picospritzer (Parker Instrumentation) set to a 40 millisecond 60 PSI ejection, delivering approximately 100-200 pL into each embryo. Embryos were allowed to recover for at least two hours at 18°C in a humidified chamber. When the embryos reached stage 5, the embryos were set up for fixing or live imaging as previously described (Frasch, 1995; McMahon et al., 2008; Supatto et al., 2009).

Double-stranded RNA (dsRNA) targeted to Pyr and Ths transcript was designed as an additional control to confirm the mesoderm migration phenotype following previously described methods (Misquitta and Paterson, 1999). The following primers were used to amplify portions of the *pyr* and *ths* cDNAs (Stathopoulos et al., 2004): *pyr*, 5′-GGATCCTAATACGACTCACTATAGGATTGCGCGGCTACAGATACT-3′ and 5′-GGATCCTAATACGACTCACTATAGGATATTTCGCCTTGATTTGCG-3′; *ths*, 5′-GGATCCTAATACGACTCACTATAGGAGATCACCTGGACAATTCCG-3′ and 5′-GGATCCTAATACGACTCACTATAGGCCGTATGGGTCTCTTCATGG-3′. dsRNA was made from PCR products using the T7 RNA polymerase.

Fixation and antibody staining

Embryos were fixed and stained using in situ, antibody or combined antibody and in situ protocols as previously described (Lehmann and Tautz, 1994; Frasch, 1995; Kosman et al., 2004). The following antibodies were used in this study: guinea pig anti-Twist (Mike Levine, UC Berkeley, USA), rabbit anti-Even skipped (Manfred Frasch, University of Erlangen, Nürnberg, Germany), rabbit anti-Beta galactosidase (Molecular Probes), mouse anti-rat CD2 (Serotec) and mouse anti-integrin-βPS (Developmental Studies Hybridoma Bank). Embryos were mounted in Permount (Fischer Scientific) for wholemount studies or embedded in acetone-araldite (Electron Microscopy Sciences) and cut with a microtome (LKB Bromna) to create 10 μm sections. Fluorescent images were obtained with a Pascal confocal microscope (Carl Zeiss).

Two photon microscopy and image analysis

Embryos were imaged as previously described (McMahon et al., 2008; Supatto et al., 2009) using a Zeiss LSM 510 inverted microscope (Carl Zeiss) at 940 nm wavelength (Chameleon Ultra laser, Coherent). At least three embryos for each of the following backgrounds were imaged and tracked: wild-type, *pyr* morpholino, *ths* morpholino, *htl*^{AB42} mutant, *pyr* and *ths* double morpholino and *mys* morpholino. In addition, one null mutant was imaged for *pyr* (*pyr*^{e02915}) and *ths* (*ths*^{e02026}/*ths*^{Df238}) to confirm that the morpholino data was consistent with the null alleles. Nuclear tracking was performed on imaging data as previous described (McMahon et al., 2008) using Imaris software (Bitplane). Data from Imaris was exported to Matlab (The Mathworks) using ImarisXT and analyzed as previously described using custom Matlab scripts (Supatto et al., 2009). Briefly, tracking data from the ectoderm was fit to a cylinder in order to convert the coordinate system used during imaging (i.e. Cartesian) into cylindrical coordinates. This allows for analysis of each movement along the corresponding body axis. A color code was applied to show the organization of the mesoderm cells as they collapse and spread along the ectoderm.

To quantify intercalation events, a customized Matlab program was created to examine each row of mesoderm cells over time. Each cell was sequentially highlighted in blue so that it could be followed during monolayer formation. A cell was counted as being stably incorporated into the monolayer if it joined the monolayer and remained through stage 11 (~130 minutes after tube collapse). Linear fits to the data from the final four time-points in Fig. 5J were performed, with the time data centered and scaled. The intercept parameters for the linear fits were then compared pair-wise by Welch's modified *t*-test. The largest *P*-value found was 0.0018.

Statistical analysis of protrusive activity

Protrusive activity was quantified by measuring the number of large protrusions (i.e. greater than one hair-like extension per cell) per image, within a length of ~60 microns across per image. The numbers were compared using Welch's *t*-test.

RESULTS

Mesoderm migration involves temporally distinct events

Mesoderm migration involves a series of complex behaviors that transform a tube of cells into a sheet of cells (Leptin and Grunewald, 1990; Wilson et al., 2005). Before migration begins, the mesoderm invaginates into the interior of the embryo via apical constriction of epithelial mesoderm cells, forming a mesoderm tube. Next, the mesoderm cells lose their epithelial characteristics and migrate toward the ectoderm (mesoderm tube collapse, Fig. 1A,B). The cells then change direction and move dorsally along the ectoderm (Fig. 1D,E). Lastly, mesoderm cells that are not in contact with the ectoderm do so, forming a monolayer (Fig. 1G,H).

Using live imaging of wild-type embryos, we explored whether the movements that encompass mesoderm migration are distinct or overlap temporally. Embryos with ubiquitously expressed H2A-GFP were imaged and mesoderm cells were tracked as previously described (Supatto et al., 2009). Tracking data was transformed into cylindrical coordinates using Matlab to fit the body plan of the embryo, so that the radial coordinate, *r*, represents cell movements from the center to the surface of the embryo, toward the ectoderm layer (e.g. collapse of the mesodermal tube and intercalation; Fig. 1C,I), and the movement along the curvature of the embryo, θ, represents motion in the angular direction, associated with the dorsoventral axis (e.g. dorsal spreading; Fig. 1F). In our previous study, we focused on decomposing the 3D movement of cells in particular directions (McMahon et al., 2008). In this work, we highlight the fact that collapse, spreading and monolayer formation are temporally distinct (Fig. 1C,F,I). We hypothesized that these movements involve different types of migratory behaviors guided by distinct molecular signals. As a result, our aim was to define the role of the genes involved in regulation of mesoderm migration within this temporal and spatial framework.

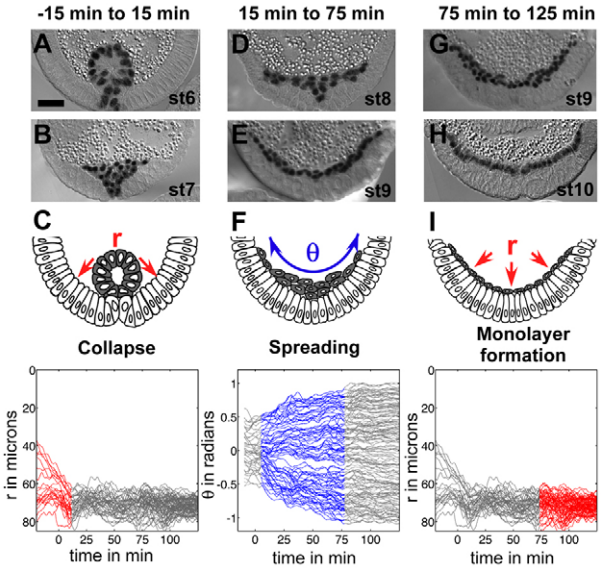

Fig. 1. Mesoderm migration is a multi-step process involving temporally distinct movements. (**A**,**B**,**D**,**E**,**G**,**H**) Embryo cross-sections stained with Twist antibody (black) to mark the mesoderm. Each stage is shown to demonstrate movement of the mesoderm over time: (A) stage 6, (B) stage 7, (D) stage 8, (E,G) stage 9 and (H) stage 10. Onset of germband elongation is represented by 0 minutes. Scale bar: 20 μm. (**C**) Collapse involves movement of mesoderm cells toward the ectoderm. Movement of mesoderm cells toward the ectoderm is represented by the radial axis of a cylinder, *r* (*y*-axis: 0=center of embryo, 90=ectoderm). The collapse of the mesoderm is shown as *r* over time, with each line representing movement of a single cell. Red is used to highlight the time period of collapse. (**F**) Spreading occurs after collapse and involves mesoderm cells crawling along the ectoderm, which is represented by the curvature of a cylinder, θ. Spreading is demonstrated by graphing θ over time (midline=0; dorsalmost points coincident with angular positions=1, –1). The timing of spreading is highlighted in blue. (**I**) Monolayer formation occurs last and involves incorporation of all cells into one layer via intercalation (see Fig. 5 for more details). Monolayer formation happens in the *r* direction from 75 minutes onward (highlighted in red).

pyramus and *thisbe* mutants display a non-monolayer phenotype

FGF signaling has been previously shown to be important for mesoderm migration. We showed recently that the preliminary function of the FGFR Heartless (Htl) is to support symmetrical collapse of the mesoderm onto the ectoderm (McMahon et al., 2008). We set out to find whether the ligands for Htl – the FGFs Pyramus (Pyr) and Thisbe (Ths) – are both required for mesoderm migration and, if so, whether they have distinct roles in migration. Pyr and Ths are expressed in dynamic patterns throughout development and have non-overlapping expression domains during mesoderm migration (Fig. 2A,B) (Gryzik and Muller, 2004; Stathopoulos et al., 2004). The *pyr* and *ths* mutant phenotypes were previously described using fixed sections. One study found that *pyr* and *ths* mutants both have a mesoderm monolayer defect (Kadam et al., 2009), whereas another claimed that only *pyr* was important for monolayer formation (Klingseisen et al., 2009), demonstrating that analysis of dynamic processes using fixed sections can be inconsistent, especially if the phenotype is variable or subtle.

We confirmed by statistical analysis of fixed sections that *pyr* and *ths* mutants do both exhibit a non-monolayer mesoderm phenotype, one weaker than that of the FGFR *htl* mutant (Fig. 2C-J; see Fig. S1 in the supplementary material). All available mutants produce similar phenotypes, with *ths* supporting a severe non-monolayer phenotype more frequently than *pyr* (Table 1; see Fig. S1 in the supplementary material). Placing a *pyr* allele over a *ths* allele was able to rescue monolayer formation, dismissing the possibility that a second site mutation contributes to the observed phenotype (see Fig. S1 in the supplementary material). In addition, we generated morpholinos and double-stranded RNAs (dsRNAs) to both *pyr* and *ths*, which produced similar phenotypes to the loss-of-function mutants (Fig. 2K-N; see Fig. S1 in the supplementary material). By analyzing several different mutant backgrounds, it is clear that both Pyr and Ths are important for mesoderm migration. We therefore used in vivo imaging to determine their precise role in this dynamic process.

In vivo imaging reveals that *thisbe* mutants have a collapse defect

We used two-photon microscopy to image *pyr* and *ths* mutants expressing ubiquitous H2A-GFP, which permits simultaneous tracking of mesoderm and ectoderm cells during gastrulation (Fig.

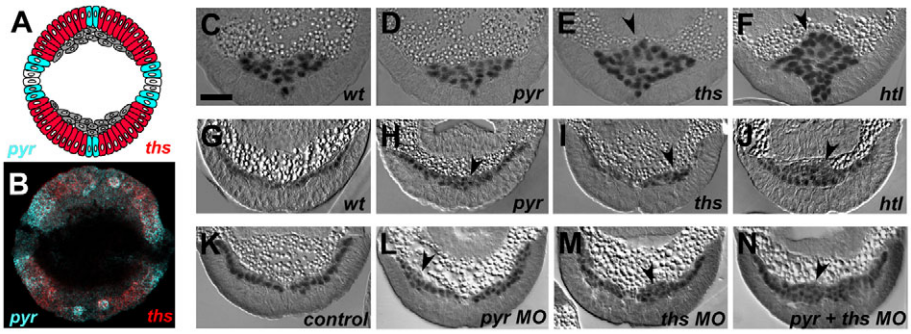

Fig. 2. *pyr* and *ths* mutants have a non-monolayer mesoderm phenotype. (**A**,**B**,**G-N**) Embryo cross-sections at stage 10. (**C-F**) Embryo cross-sections at stage 7. (A) Schematic of Pyr (blue) and Ths (red) expression in the ectoderm during mesoderm spreading. The receptor Htl is found in the mesoderm (gray). (B) Expression patterns of *pyr* (blue) and *ths* (red) transcript during mesoderm spreading detected by in situ hybridization. (C-J) Embryos of indicated genetic backgrounds sectioned and stained with anti-Twist antibody (black) in wild-type (C,G), pyr^{e02915} (D,H), ths^{e02026}/ths^{Df238} (E,I) and htl^{AB42} (F,J) mutants. Arrowheads highlight defects. Morpholinos (MOs) were injected for live imaging purposes (see Materials and methods). Injection of *gal4* MO (K), which does not have a target in *Drosophila*, did not affect mesoderm spreading, whereas injection of *pyr* MO (L) and *ths* MO (M) produced phenotypes similar to the genetic mutants. (N) Injection of *pyr* and *ths* MO together produced a phenotype similar to *htl* mutants. Scale bar: 20 μm.

3A-D) (McMahon et al., 2008). This permitted us to decompose the migration into different types of movements and to decipher the subtle non-monolayer phenotypes.

To facilitate more efficient live imaging, we utilized translation blocking morpholinos (MOs) designed against *pyr* and *ths* transcripts to reduce the number of imaging sessions required to obtain mutant data; when assaying embryos of zygotic recessive mutant backgrounds, only one of four embryos was a homozygous mutant, whereas each morpholino injected embryo displayed the expected phenotype. Morpholinos injected into pre-cellularized embryos were able to reproduce the *pyr* and *ths* phenotypes of loss-of-function alleles (Fig. 2K-M; see Fig. S1G in the supplementary material). In addition, co-injection of *pyr* and *ths* morpholinos supported a mutant phenotype that was more severe and comparable to that of *htl* mutants (compare Fig. 2J with 2N) as well as the mutant background *Df(2R)BSC25*, which removes both *pyr* and *ths* genes (data not shown) (Stathopoulos et al., 2004).

We imaged both morpholino and null mutants for Pyr and Ths (see Materials and methods) and tracked a subset of mesoderm cells over time using Imaris software (see Movies 1 and 2 in the supplementary material). As with wild-type embryos (see Fig. 1), tracking data was converted into cylindrical coordinates to fit the body plan of the embryo (Fig. 4A). When the movement was decomposed into r and θ, it revealed that *ths* mutants, like previously characterized *htl* mutants, have a mesoderm tube collapse defect in which cells from the uppermost part of the tube fail to migrate toward the ectoderm (blue lines, Fig. 4B-C,E,G). In *htl* mutants, tube collapse was asymmetrical, with the tube falling either toward the left or right half of the embryo, resulting in an indirect migratory defect along θ (Fig. 4D,F) (McMahon et al., 2008). Unlike in *htl* mutants, however, movement in the angular direction was at worst very mildly affected in a few cells in *ths* mutants, suggesting that Pyr can keep the collapse symmetrical in the absence of Ths (Fig. 4H). *pyr* mutants displayed little to no defects along r or θ (Fig. 4I,J), which suggests that Ths is able to support mesodermal tube collapse in the absence of Pyr.

Table 1. Percent of embryos with a mesoderm monolayer at stage 10

Genotype	% embryos with monolayer (*n*=number of embryos scored)
wild-type	84.6 (*n*=13)
pyr^{e02915}	42.8 (*n*=11)
ths^{e02026}/Df238	25.0 (*n*=12)
htl^{AB42}	0 (*n*=7)
DFBSC25	0 (*n*=10)
gal4 MO	88.9 (*n*=18)
pyr MO	45.5 (*n*=11)
ths MO	27.3 (*n*=11)
pyr + *ths* MO	11.1 (*n*=18)

MO=morpholino.

Quantitative analysis shows that *pyr* and *ths* mutants both display intercalation defects

To further characterize the non-monolayer phenotype of *pyr* and *ths* mutants, we focused on the small cell movements and rearrangements found in intercalation, as the non-monolayer in *pyr* mutants cannot be accounted for by a collapse defect. In this particular case, we investigated whether intercalation events might support the generation of the mesoderm monolayer during gastrulation (Fig. 5A). We quantified the rate and number of intercalation events in wild-type and mutant backgrounds to see whether mesoderm intercalation is dependent on FGF signaling and whether the timing of intercalation corresponds with monolayer formation. Monolayer formation occurs during stage 9 and 10 and involves the transformation of a multi-layer into a single cell layer (~80-90 minutes into migration; Fig. 5B,C).

By focusing on the position of mesoderm cells during stage 9 and 10 (gray spots in Fig. 5), it was apparent that a subset of cells is not incorporated into the monolayer in *pyr*, *ths* and *htl* mutants (Fig. 5D-I, arrowheads). We used the tracking data from each mutant to examine the timing and number of intercalation events. We found that *pyr* has a reduced number of intercalation events compared with wild-type, that *ths* mutants have even less intercalation events than *pyr*, and that *htl* mutants have the fewest events (Fig. 5J; number of cells assayed was 303, 241, 262 and 213 for wild-type, *pyr*, *ths* and *htl*, respectively, with $P<0.002$ in all cases). Together, these data suggest that the presence of FGFs throughout the ectoderm is important for intercalation of all mesoderm cells to form a monolayer. The defects did not

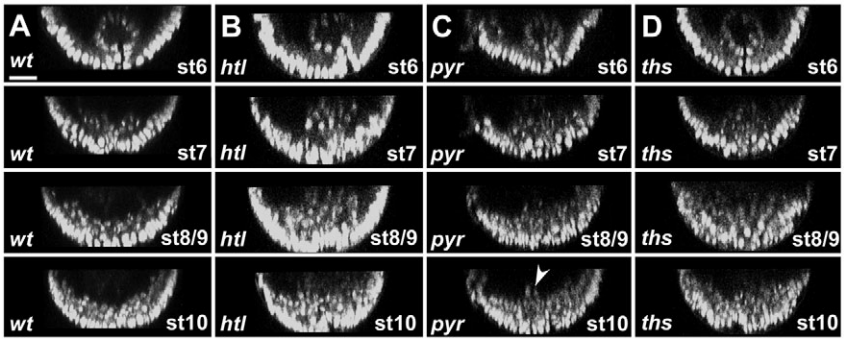

Fig. 3. Live imaging of FGF mutants using two-photon microscopy. Virtual cross-sections of H2A-GFP-expressing embryos taken from 4D imaging data sets (3D plus time) obtained on a two-photon microscope (see Materials and methods for details). (**A**) Wild-type embryos undergo characteristic movements: invagination at stage 6, collapse of the mesodermal tube at stage 7, spreading at stage 8 and 9 and monolayer formation at stage 10. (**B**) *htl* mutant embryo at stages 6-10. *htl* mutants have a collapse defect at stage 7 and a severe non-monolayer at stage 10. (**C**) *pyr* mutant embryo at stages 6-10. *pyr* mutant embryos undergo normal collapse and spreading during stages 6-9. A subset of cells are observed outside the monolayer at stage 10 (arrowhead). (**D**) *ths* mutant embryo at stages 6-10. In *ths* mutants, collapse is defective at stage 7 and a severe non-monolayer is observed at stage 10. Scale bar: 20 μm.

necessarily correspond with the particular expression pattern of each ligand. This is not surprising as ligands, including Fgf8, might have non-autonomous effects due to diffusion (e.g. Yu et al., 2009).

It has been previously shown that Htl, Pyr and Ths can influence cellular projections during collapse and spreading (Schumacher et al., 2004; Wilson et al., 2005; Klingseisen et al., 2009). As migratory defects often coincide with a failure to regulate cell shape changes and protrusive activity (McDonald et al., 2008), we examined whether the ligands control cell shape changes that might also be important for movement during monolayer formation. We visualized the protrusions using *twist* promoter-supported expression of CD2, a cell-surface protein not native to *Drosophila*, which permits examination of cell extensions exclusively in the mesoderm during stage 9 and 10 (Twist-CD2) (Dunin-Borkowski and Brown, 1995). We found that, as previously published, the leading edge is affected at stage 9, as cells fail to polarize in embryos lacking both Pyr and Ths or in *pyr* single mutants (see Fig. S2A-C in the supplementary material, arrow), but not in *ths* single mutants (see Fig. S2D in the supplementary material) (Klingseisen et al., 2009). Similar effects were observed when the ligands were ectopically expressed in the mesoderm: overexpression of *pyr* leads to

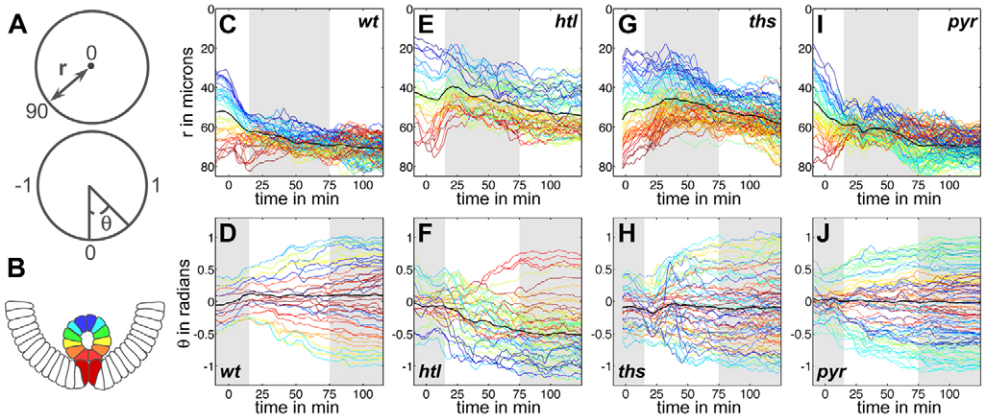

Fig. 4. Live imaging and nuclear tracking reveals defects in *ths* mutants. (**A**) *Drosophila* embryos are roughly cylindrically shaped such that movement of mesoderm cells along the dorsoventral axis can be represented by the curve of a cylinder, θ (0=midline). Movement along the radial axis *r* represents movement of mesoderm cells toward or away from the ectoderm (0=center of embryo). (**B**) A color code is applied to track the progress of each cell over time, with a color assignment given at stage 6 and retained throughout migration. The color code is along the radial axis, where red represents mesoderm cells closest to the ectoderm at stage 6 and blue represents the furthest mesoderm cells. (**C**,**E**,**G**,**I**) Collapse of the mesodermal tube as shown by a graph of *r* over time; each curve represents the movement of one cell (*y*-axis: 0=center of embryo, 90=ectoderm; the black line is the average of all tracks). White boxes highlight the time intervals of collapse and intercalation in wild-type embryos defined in Fig. 1. (C) Wild-type embryos undergo collapse of the mesodermal tube to flatten along the ectoderm. Mesoderm cells in *htl* mutants (E) and *ths* mutants (G) fail to collapse. (I) *pyr* mutants display no collapse defect. (**D**,**F**,**H**,**J**) Spreading of mesoderm cells away from the midline (0) toward the dorsalmost point of the embryo (1 or –1) is shown by graphs of θ over time. The black line is the average of all tracks. White boxes highlight the time intervals of spreading in wild-type embryos as defined in Fig. 1. (D) Wild-type mesoderm cells spread directionally away from the midline toward the dorsal-most point in the embryo, whereas *htl* mutants (F) have aberrant spreading behavior, with some cells crossing over the midline and spreading in the wrong direction. *ths* (H) and *pyr* (J) mutants spread directionally away from the midline toward dorsal regions.

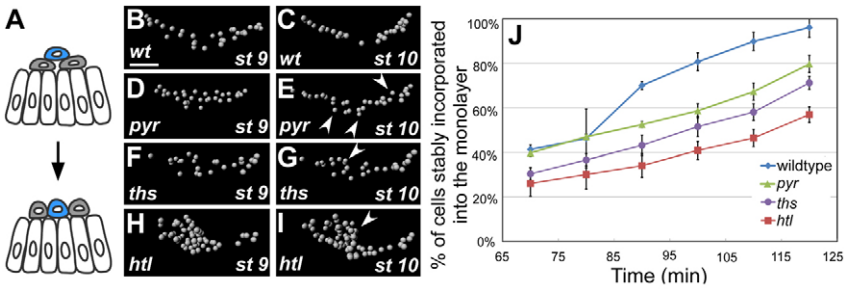

Fig. 5. Intercalation of mesoderm cells during monolayer formation is disrupted in FGF mutants. (**A**) Intercalation occurs during mesoderm migration when a cell that is not in contact with the ectoderm (blue) moves toward the ectoderm. (**B-I**) A subset of mesoderm cells are tracked from stage 9 (B,D,F,H) to 10 (C,E,G,I) (gray ball=mesoderm cell), showing how cells go from a multilayer to a monolayer in wild-type embryos (B,C) but not in *pyr* (D,E), *ths* (F,G) or *htl* (H,I) mutants. Arrowheads demonstrate cells that have not intercalated. The view shown is similar to a cross-section as in Fig. 2. (**J**) A graph of stable intercalation of mesoderm cells over time. The number of cells that intercalate stably into the monolayer is highest for wild-type embryos, whereas *pyr*, *ths* and *htl* mutants have successively lower numbers of intercalating cells. The differences between pairs of phenotypes are all statistically significant ($P<0.002$). Scale bar: 20 μm.

severe loss of cellular extensions, whereas overexpression of *ths* has a minor effect (see Fig. S2E-F in the supplementary material) (Klingseisen et al., 2009).

Conversely, it had not been examined previously whether mesoderm cells extend protrusions toward the ectoderm during monolayer formation. We found that, in the *pyr*/*ths* double mutant, mesoderm cells extend fewer large protrusions into the ectoderm than in wild-type embryos (see Fig. S2A,B in the supplementary material, arrowheads). Mesoderm sections from double-mutant embryos contained 4.0±0.8 protrusions per image (n=11), whereas those from wild-type exhibited 7.7±0.9 protrusions (n=11, $P<0.01$). *pyr* and *ths* single mutants also failed to extend as many protrusions into the ectoderm as wild-type (see Fig. S2C,D in the supplementary material; 4.3±0.9 and 4.8±1.5, respectively, n=9 for each; $P<0.01$ for each compared with wild-type). These data suggest that protrusive activity might be important for monolayer formation and provide insights into the mechanism by which FGF signaling might control radial intercalation.

Myospheroid activity is required for monolayer formation and is controlled by Rap1

After characterization of the FGF mutants, we screened for other genes that produce similar phenotypes to the FGF mutants using fixed section analysis. To this end, we discovered that embryos mutant for the GTPase Rap1 have collapse and monolayer formation defects similar to those mutant for Htl (Fig. 6A-C,E-G). However, *Rap1* mutants also exhibit defects in ventral furrow formation and germband elongation, making the interpretation of its primary roles in mesoderm migration difficult (Roote and Zusman, 1995; Asha et al., 1999). Therefore, we sought out targets of Rap1 that displayed more-specific mesoderm migration defects.

Several studies suggest that Rap1 is required for activation of integrins at the cell membrane, which in turn is required for cell adhesion and migration (for a review, see Bos, 2005; Boettner and Van Aelst, 2009; Vicente-Manzanares et al., 2009). This led us to explore the role of integrins during mesoderm migration in *Drosophila*. There are two beta integrin subunits in *Drosophila*, but only the βPS subunit, Myospheroid (Mys), is expressed during mesoderm migration, in between the mesoderm and ectoderm at stage 9 and 10 (see Fig. S3A-F in the supplementary material) (Leptin et al., 1989; Gotwals et al., 1994).

We found that *mys* mutants exhibit a non-monolayer mesoderm defect at stage 9 and 10 in fixed sections (Fig. 6D,H). Surprisingly, we found that Mys localization is affected in both *htl* and *Rap1* mutants, with gaps and reduced expression of Mys in *htl* mutants and a total absence of Mys in *Rap1* mutants (Fig. 6I-K). These results suggest that Mys plays a specific and crucial role during monolayer formation and that Mys expression might be regulated, at least in part, by FGF signaling. This result also suggests the possibility that FGF signaling functions during mesoderm migration and spreading to regulate cell adhesion (see Discussion). To definitively test the role of Mys in intercalation, we dissected the phenotype using quantitative imaging methods.

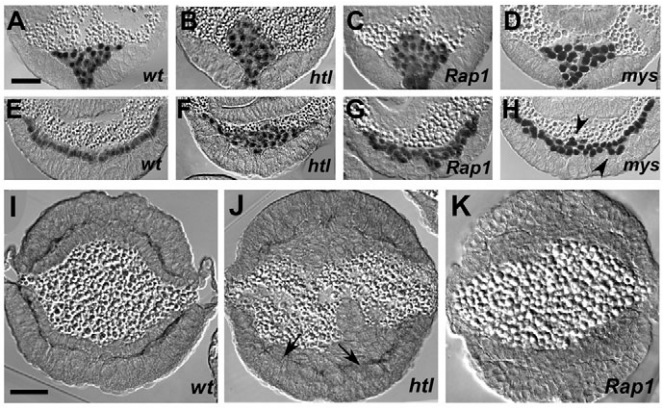

Fig 6. Rap1 and Mys are required for monolayer formation. (A-H) Cross sections of embryos stained with Twist antibody (black). (A-D) Stage 7 embryos and (E-H) stage 10 embryos. (**A**,**E**) Wild-type embryos undergo tube collapse at stage 7 (A) and then intercalation to form a monolayer during stage 10 (E). (**B-D**,**F-H**) In *htl* mutants (B) and *Rap1* mutants (C), tube collapse is defective, resulting in a clump of cells at stage 7. Intercalation is also affected, resulting in the lump remaining at stage 10 (F,G). In *mys* mutants, tube collapse is normal, resulting in normal mesoderm behavior at stage 7 (D). During stage 10, a non-monolayer is observed (H, arrowheads). (**I-K**) Cross-sections of embryos at stage 10 stained with Mys antibody (black). (I) In wild-type embryos, Mys is expressed at the boundary between the mesoderm and ectoderm. (J) In *htl* mutants, Mys levels are reduced and gaps in expression are observed (arrows). (K) *Rap1* mutant embryos fail to localize Mys at the ectoderm-mesoderm boundary. Scale bars: 20 μm.

Myospheroid mutants exhibit a decrease in intercalation events during mesoderm migration

We performed live imaging on H2A-GFP embryos injected with a translation blocking morpholino designed against the *mys* transcript (see Fig. S3G-J in the supplementary material). The Mys morpholino was able to reproduce the phenotype of the genetic null mutant and also eliminate Mys protein expression in the embryo (see Fig. S3K,L in the supplementary material). We tracked a subset of mesoderm cells from *mys* mutant imaging data and analyzed movement in r and θ (see Movie 3 in the supplementary material). We found that neither collapse (r) nor spreading (θ) is affected by loss of Mys (Fig. 7A,B). Like the FGF ligand mutants, we found a reduced number of intercalation events during monolayer formation in *mys* mutants compared with wild-type (Fig. 7C,F,G; 90 cells were assayed for *mys* mutants, $P<0.05$). We also found that mesoderm membrane protrusions into the ectoderm were completely absent in *mys* mutants during the same time interval as monolayer formation (i.e. stage 9 and 10), which could be contributing to the observed intercalation defects (Fig. 7D,E; see Fig. S2G,H in the supplementary material). Our data indicate that Mys is important for monolayer formation and provide support for the view that this migratory event is molecularly distinct from earlier events, as ventral furrow formation, collapse and spreading are unaffected in *mys* mutants.

DISCUSSION

Mesoderm migration is composed of a series of movements in different directions

Mesoderm migration in *Drosophila* is a combination of complex three-dimensional movements involving many molecular components. We have demonstrated here that live imaging, coupled with quantitative analyses, is important for studying complex cell movements, as it allowed us to decompose migration into different movement types and thus to describe subtle phenotypes. First, we extended analysis of the directional movements of mesoderm cells within wild-type embryos, focusing on the temporal sequences of events. We found that cells follow a sequential and distinct set of trajectories: movement in the radial direction (tube collapse: –5 to 15 minutes, 0=onset of germband elongation), followed by movement in the angular direction (dorsal migration: 15 to 75 minutes) and ending with small intercalation movements in the radial direction (monolayer formation: 75 to 110 minutes). These movements appear temporally distinct (i.e. stepwise), and thus we searched for molecular signals controlling each process.

FGF signaling controls tube collapse and intercalation to specify a monolayer

We investigated which mesoderm movements were FGF-dependent and, in particular, either Ths- or Pyr-dependent. The interaction between Htl and its two ligands provides a simpler system relative to vertebrates (which exhibit over 120 receptor-ligand interactions) in which to study how and why multiple FGF ligands interact with the same receptor. Previously, we had found that FGF signaling via the Htl FGFR controls collapse of the mesodermal tube but not dorsal-directed spreading (McMahon et al., 2008). Here we demonstrated that FGF signaling is also required for monolayer formation. In addition, we defined distinct, non-redundant roles for the FGF ligands: Ths (but not Pyr) is required for collapse of the mesodermal tube, whereas both Pyr and Ths are required for proper intercalation of mesoderm cells after dorsal spreading.

This analysis raises questions about ligand choice during collapse and monolayer formation. Within the mesodermal tube, cells at the top require a long-range signal in order to orient towards the ectoderm during tube collapse, whereas the signals controlling intercalation during monolayer formation can be of shorter range. We suggest that the ligands have different activities that are appropriately tuned for these processes. In fact, recent studies of the functional domains of these proteins suggest that Ths has a longer range of action than Pyr (S. Tulin and A.S., unpublished results), in agreement with our analysis that Pyr does not support tube collapse, but does have a hand in monolayer formation.

Rap1 and Myospheroid are required for monolayer formation

We have demonstrated here that *Rap1* mutants have a similar mesoderm phenotype to the FGFR *htl* mutant, with defects in collapse and monolayer formation. We were unable to establish whether Rap1 acts downstream of FGF signaling, as the complete

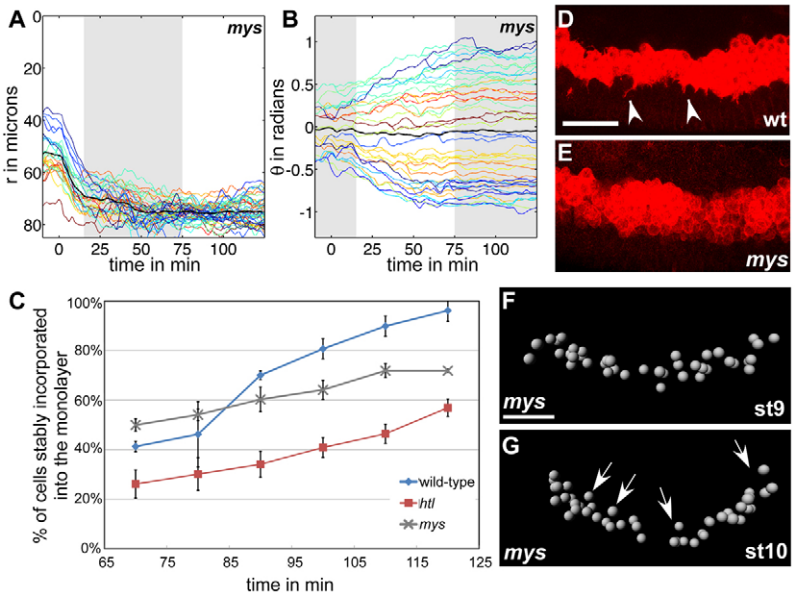

Fig. 7. Mys is required for monolayer formation and mesoderm cell shape changes. (**A**,**B**) Collapse and spreading of mesoderm cells in *mys* mutants represented by r and θ over time, respectively (see Fig. 4 for more details). A radial color code is applied to distinguish each cell track over time. The black line represents the average behavior of all mesoderm cells. (**C**) Monolayer formation is measured as the percent of cells that are incorporated by stable intercalation into the monolayer over time. *mys* mutants exhibit a lower number of intercalation events than wild-type embryos, but a higher number than *htl* mutants. (**D**,**E**) Lateral projections of stage 9 Twist-CD2 embryos stained with CD2 antibody, which marks cellular protrusions in the mesoderm. (D) Wild-type mesoderm cells extend membrane protrusions into the ectoderm during monolayer formation (arrowheads). (E) *mys* mutants exhibit rounded mesoderm cells with no protrusions into the ectoderm. (**F**,**G**) A subset of mesoderm cells are tracked from stage 9 (F) to 10 (G) (gray ball=mesoderm cell). The view shown is similar to a cross-section like in Fig. 2. Arrows indicate cells not intercalating into the monolayer. Scale bars: 20 μm.

loss of Mys in *Rap1* mutants is more severe than the patchy expression of Mys seen in *htl* mutants. Therefore, Rap1 could be working in parallel to or downstream of FGF signaling during mesoderm migration. Rap1 has been implicated in several morphogenetic events during *Drosophila* gastrulation and probably interacts with many different signaling pathways (Roote and Zusman, 1995; Asha et al., 1999). Further study of Rap1, along with other GTPases, will shed light onto their role during mesoderm migration, how they interact with one another and what signaling pathways control them.

We chose to focus on the more-specific phenotype of *mys* mutants, as its localization is affected in *htl* mutants and it exhibits a monolayer defect that is similar to *pyr* and *ths* mutants. Integrins are important for cell adhesion, so it is not surprising that cells fail to make stable contact with the ectoderm through intercalation in *mys* mutants. However, some cells do contribute to monolayer formation in the absence of Mys, implying that other adhesion molecules are involved in maintaining contact between the mesoderm and ectoderm. These other adhesion molecules might be activated downstream of FGF signaling as the *htl* mutant monolayer phenotype is more severe than the *mys* mutant. Discovering the downstream targets of Htl, which we suggest might regulate cell adhesion properties, will help to shed light on the mechanisms supporting collapse of the mesodermal tube (which is not dependent on Mys) and monolayer formation (which is Mys-dependent).

Cell shape changes are important for monolayer formation

Cell protrusions, such as filopodia, are important for sensing chemoattractants and polarizing movement during migration (for a review, see Mattila and Lappalainen, 2008). Previous studies have focused on protrusive activity at the leading edge during mesoderm migration in *Drosophila* and shown that these protrusions are FGF-dependent (Schumacher et al., 2004; Klingseisen et al., 2009). In this study, we have found that protrusions exist in all mesoderm cells, not just the leading edge, and that these protrusions also extend into the ectoderm.

Our study demonstrates that FGF signaling, as well as integrin activity, is required to support protrusive activity into the ectoderm; this is a potential mechanism by which FGF signaling and Mys could control movement toward the ectoderm during monolayer formation. The function of protrusions at the leading edge remains unclear, as they appear to be reduced in *pyr* and *mys* mutants (see Fig. S2 in the supplementary material), but migration in the dorsal direction still occurs in both mutant backgrounds. One interpretation is that FGF and Mys are important for generalized protrusive activity and that extensive protrusions are required for intercalation but not dorsal migration.

Mesoderm migration involves four distinct steps

Based on our study, we propose that mesoderm migration is a stepwise process, with each event requiring different molecular cues to achieve collective migration (Fig. 8). Invagination of the mesoderm is the first step in this process and is dependent on Snail, Twist, Concertina, Fog and several other genes (Parks and Wieschaus, 1991; Reuter and Leptin, 1994; Morize et al., 1998; Aracena et al., 2006; Seher et al., 2007; Martin et al., 2009). Next, collapse of the mesoderm tube onto the ectoderm requires Htl activation via Ths. Rap1 might be involved in this process as well but the phenotype of *Rap1* mutants is complex and it is unclear which phenotypes are primary defects (see Fig. 6C,G) (Roote and Zusman, 1995; Asha et al., 1999).

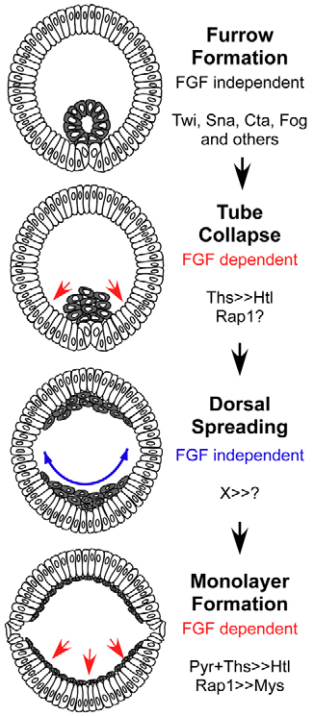

Fig. 8. Multi-step model of mesoderm migration. Formation of the ventral furrow occurs first during gastrulation. This process depends on many inputs, such as Twist, Snail, Concertina and Fog. Following furrow and tube formation, the mesoderm collapses onto the ectoderm, which is dependent on FGF signaling through Thisbe. Rap1 might also be involved. Subsequently, directed dorsal spreading occurs, and it appears to be independent of FGF signaling. Lastly, monolayer formation by intercalation is FGF-dependent and requires both ligands. Rap1 controls Mys, which in turn is required for monolayer formation.

Following collapse, mesoderm cells spread dorsally by an unknown mechanism. Dorsal migration is unaffected in *pyr* and *ths* mutants and occurs in all cells that contact the ectoderm in *htl* mutants, implying that FGF signaling is, at most, indirectly involved in this step owing to the earlier tube collapse defect (McMahon et al., 2008). Whether dorsal migration requires chemoattractive signals or whether the cells simply move in this direction because it is the area of least resistance remains unclear.

Finally, after dorsal spreading is complete, any remaining cells not contacting the ectoderm intercalate to form a monolayer. This process is controlled by a combination of both Pyr and Ths interacting through Htl and also by Rap1 and Mys. In other systems, intercalation can lead to changes in the properties of the cell collective, for instance, lengthening of a body plan (Keller, 2006). However, we have shown here that dorsal migration and spreading are not a result of intercalation, as intercalation occurs after spreading has finished (Fig. 5).

Coordination of these signals to control collective migration enables the mesoderm to form a symmetrical structure, which is essential for embryo survival. This model begins to address the question of how hundreds of cells move in concerted fashion and is relevant for a generalized understanding of embryogenesis and organogenesis. We find that mesoderm migration is accomplished through sequential movements in different directions, implying that collective migration might be best achieved by distinct phases of movement.

Acknowledgements
We thank Manfred Frasch, Iswar Hariharan, Maria Leptin, Mike Levine and Arno Müller for providing fly stocks and antibodies. We also thank the Caltech Biological Imaging Center for use of their microscopes. This work was supported by grants to A.S. from the NIH (R01 GM078542), and in part by a grant from the Jane Coffin Childs Memorial Fund for Medical Research as G.T.R. is a fellow of the Jane Coffin Childs Memorial Fund for Medical Research. Deposited in PMC for release after 12 months.

Competing interests statement
The authors declare no competing financial interests.

Supplementary material
Supplementary material for this article is available at
http://dev.biologists.org/lookup/suppl/doi:10.1242/dev.051573/-/DC1

References
Aracena, J., Gonzalez, M., Zuniga, A., Mendez, M. A. and Cambiazo, V. (2006). Regulatory network for cell shape changes during *Drosophila* ventral furrow formation. *J. Theor. Biol.* **239**, 49-62.
Asha, H., de Ruiter, N. D., Wang, M. G. and Hariharan, I. K. (1999). The Rap1 GTPase functions as a regulator of morphogenesis in vivo. *EMBO J.* **18**, 605-615.
Beiman, M., Shilo, B. Z. and Volk, T. (1996). Heartless, a *Drosophila* FGF receptor homolog, is essential for cell migration and establishment of several mesodermal lineages. *Genes Dev.* **10**, 2993-3002.
Boettner, B. and Van Aelst, L. (2009). Control of cell adhesion dynamics by Rap1 signaling. *Curr. Opin. Cell Biol.* **21**, 684-693.
Bos, J. L. (2005). Linking Rap to cell adhesion. *Curr. Opin. Cell Biol.* **17**, 123-128.
Brown, N. H. (2000). Cell-cell adhesion via the ECM: integrin genetics in fly and worm. *Matrix Biol.* **19**, 191-201.
Carmona, G., Gottig, S., Orlandi, A., Scheele, J., Bauerle, T., Jugold, M., Kiessling, F., Henschler, R., Zeiher, A. M., Dimmeler, S. et al. (2009). Role of the small GTPase Rap1 for integrin activity regulation in endothelial cells and angiogenesis. *Blood* **113**, 488-497.
Chou, T. B. and Perrimon, N. (1996). The autosomal FLP-DFS technique for generating germline mosaics in *Drosophila melanogaster*. *Genetics* **144**, 1673-1679.
Deisboeck, T. S. and Couzin, I. D. (2009). Collective behavior in cancer cell populations. *BioEssays* **31**, 190-197.
Delon, I. and Brown, N. H. (2007). Integrins and the actin cytoskeleton. *Curr. Opin. Cell Biol.* **19**, 43-50.
Dunin-Borkowski, O. M. and Brown, N. H. (1995). Mammalian CD2 is an effective heterologous marker of the cell surface in Drosophila. *Dev. Biol.* **168**, 689-693.
Franzdottir, S. R., Engelen, D., Yuva-Aydemir, Y., Schmidt, I., Aho, A. and Klambt, C. (2009). Switch in FGF signalling initiates glial differentiation in the *Drosophila* eye. *Nature* **460**, 758-761.
Frasch, M. (1995). Induction of visceral and cardiac mesoderm by ectodermal Dpp in the early *Drosophila* embryo. *Nature* **374**, 464-467.
Friedl, P. and Gilmour, D. (2009). Collective cell migration in morphogenesis, regeneration and cancer. *Nat. Rev. Mol. Cell Biol.* **10**, 445-457.
Gisselbrecht, S., Skeath, J. B., Doe, C. Q. and Michelson, A. M. (1996). heartless encodes a fibroblast growth factor receptor (DFR1/DFGF-R2) involved in the directional migration of early mesodermal cells in the *Drosophila* embryo. *Genes Dev.* **10**, 3003-3017.
Gotwals, P. J., Paine-Saunders, S. E., Stark, K. A. and Hynes, R. O. (1994). *Drosophila* integrins and their ligands. *Curr. Opin. Cell Biol.* **6**, 734-739.
Gryzik, T. and Muller, H. A. (2004). FGF8-like1 and FGF8-like2 encode putative ligands of the FGF receptor Htl and are required for mesoderm migration in the *Drosophila* gastrula. *Curr. Biol.* **14**, 659-667.
Huelsmann, S., Hepper, C., Marchese, D., Knoll, C. and Reuter, R. (2006). The PDZ-GEF dizzy regulates cell shape of migrating macrophages via Rap1 and integrins in the *Drosophila* embryo. *Development* **133**, 2915-2924.
Ilina, O. and Friedl, P. (2009). Mechanisms of collective cell migration at a glance. *J. Cell Sci.* **122**, 3203-3208.
Jeon, T. J., Lee, D. J., Lee, S., Weeks, G. and Firtel, R. A. (2007). Regulation of Rap1 activity by RapGAP1 controls cell adhesion at the front of chemotaxing cells. *J. Cell Biol.* **179**, 833-843.
Kadam, S., McMahon, A., Tzou, P. and Stathopoulos, A. (2009). FGF ligands in *Drosophila* have distinct activities required to support cell migration and differentiation. *Development* **136**, 739-747.
Keller, R. (2006). Mechanisms of elongation in embryogenesis. *Development* **133**, 2291-2302.
Klingseisen, A., Clark, I. B., Gryzik, T. and Muller, H. A. (2009). Differential and overlapping functions of two closely related *Drosophila* FGF8-like growth factors in mesoderm development. *Development* **136**, 2393-2402.
Kooistra, M. R., Dube, N. and Bos, J. L. (2007). Rap1: a key regulator in cell-cell junction formation. *J. Cell Sci.* **120**, 17-22.
Kosman, D., Mizutani, C. M., Lemons, D., Cox, W. G., McGinnis, W. and Bier, E. (2004). Multiplex detection of RNA expression in *Drosophila* embryos. *Science* **305**, 846.
Lecaudey, V. and Gilmour, D. (2006). Organizing moving groups during morphogenesis. *Curr. Opin. Cell Biol.* **18**, 102-107.
Lehmann, R. and Tautz, D. (1994). In situ hybridization to RNA. *Methods Cell Biol.* **44**, 575-598.
Leptin, M. and Grunewald, B. (1990). Cell shape changes during gastrulation in *Drosophila*. *Development* **110**, 73-84.
Leptin, M., Bogaert, T., Lehmann, R. and Wilcox, M. (1989). The function of PS integrins during *Drosophila* embryogenesis. *Cell* **56**, 401-408.
Martin, A. C., Kaschube, M. and Wieschaus, E. F. (2009). Pulsed contractions of an actin-myosin network drive apical constriction. *Nature* **457**, 495-499.
Mattila, P. K. and Lappalainen, P. (2008). Filopodia: molecular architecture and cellular functions. *Nat. Rev. Mol. Cell Biol.* **9**, 446-454.
McDonald, J. A., Khodyakova, A., Aranjuez, G., Dudley, C. and Montell, D. J. (2008). PAR-1 kinase regulates epithelial detachment and directional protrusion of migrating border cells. *Curr. Biol.* **18**, 1659-1667.
McMahon, A., Supatto, W., Fraser, S. E. and Stathopoulos, A. (2008). Dynamic analyses of *Drosophila* gastrulation provide insights into collective cell migration. *Science* **322**, 1546-1550.
Misquitta, L. and Paterson, B. M. (1999). Targeted disruption of gene function in *Drosophila* by RNA interference (RNA-i): a role for nautilus in embryonic somatic muscle formation. *Proc. Natl. Acad. Sci. USA* **96**, 1451-1456.
Montell, D. J. (2008). Morphogenetic cell movements: diversity from modular mechanical properties. *Science* **322**, 1502-1505.
Mori, S., Wu, C. Y., Yamaji, S., Saegusa, J., Shi, B., Ma, Z., Kuwabara, Y., Lam, K. S., Isseroff, R. R., Takada, Y. K. et al. (2008). Direct binding of integrin alphavbeta3 to FGF1 plays a role in FGF1 signaling. *J. Biol. Chem.* **283**, 18066-18075.
Morize, P., Christiansen, A. E., Costa, M., Parks, S. and Wieschaus, E. (1998). Hyperactivation of the folded gastrulation pathway induces specific cell shape changes. *Development* **125**, 589-597.
Murray, M. J. and Saint, R. (2007). Photoactivatable GFP resolves *Drosophila* mesoderm migration behaviour. *Development* **134**, 3975-3983.
O'Reilly, A. M., Lee, H. H. and Simon, M. A. (2008). Integrins control the positioning and proliferation of follicle stem cells in the *Drosophila* ovary. *J. Cell Biol.* **182**, 801-815.
Parks, S. and Wieschaus, E. (1991). The *Drosophila* gastrulation gene concertina encodes a G alpha-like protein. *Cell* **64**, 447-458.
Reedquist, K. A., Ross, E., Koop, E. A., Wolthuis, R. M., Zwartkruis, F. J., van Kooyk, Y., Salmon, M., Buckley, C. D. and Bos, J. L. (2000). The small GTPase, Rap1, mediates CD31-induced integrin adhesion. *J. Cell Biol.* **148**, 1151-1158.
Reuter, R. and Leptin, M. (1994). Interacting functions of snail, twist and huckebein during the early development of germ layers in *Drosophila*. *Development* **120**, 1137-1150.
Roote, C. E. and Zusman, S. (1995). Functions for PS integrins in tissue adhesion, migration, and shape changes during early embryonic development in *Drosophila*. *Dev. Biol.* **169**, 322-336.
Rorth, P. (2007). Collective guidance of collective cell migration. *Trends Cell Biol.* **17**, 575-579.
Rorth, P. (2009). Collective cell migration. *Annu. Rev. Cell Dev. Biol.* **25**, 407-429.
Schumacher, S., Gryzik, T., Tannebaum, S. and Muller, H. A. (2004). The RhoGEF Pebble is required for cell shape changes during cell migration triggered by the *Drosophila* FGF receptor Heartless. *Development* **131**, 2631-2640.
Seher, T. C., Narasimha, M., Vogelsang, E. and Leptin, M. (2007). Analysis and reconstitution of the genetic cascade controlling early mesoderm morphogenesis in the *Drosophila* embryo. *Mech. Dev.* **124**, 167-179.
Stathopoulos, A., Tam, B., Ronshaugen, M., Frasch, M. and Levine, M. (2004). pyramus and thisbe: FGF genes that pattern the mesoderm of *Drosophila* embryos. *Genes Dev.* **18**, 687-699.
Supatto, W., McMahon, A., Fraser, S. E. and Stathopoulos, A. (2009). Quantitative imaging of collective cell migration during *Drosophila* gastrulation: multiphoton microscopy and computational analysis. *Nat. Protoc.* **4**, 1397-1412.
Thisse, B. and Thisse, C. (2005). Functions and regulations of fibroblast growth factor signaling during embryonic development. *Dev. Biol.* **287**, 390-402.
Vicente-Manzanares, M., Choi, C. K. and Horwitz, A. R. (2009). Integrins in cell migration-the actin connection. *J. Cell Sci.* **122**, 199-206.
Weijer, C. J. (2009). Collective cell migration in development. *J. Cell Sci.* **122**, 3215-3223.
Wilson, R. and Leptin, M. (2000). Fibroblast growth factor receptor-dependent morphogenesis of the *Drosophila* mesoderm. *Philos. Trans. R. Soc. Lond. B Biol. Sci.* **355**, 891-895.
Wilson, R., Vogelsang, E. and Leptin, M. (2005). FGF signalling and the mechanism of mesoderm spreading in *Drosophila* embryos. *Development* **132**, 491-501.
Yu, S. R., Burkhardt, M., Nowak, M., Ries, J., Petrasek, Z., Scholpp, S., Schwille, P. and Brand, M. (2009). Fgf8 morphogen gradient forms by a source-sink mechanism with freely diffusing molecules. *Nature* **461**, 533-536.